



# Polymerization of ethylene to branched polyethylene with silica and Merrifield resin supported nickel(II) catalysts with $\alpha$ -diimine ligands

Yan-Guo Li, Li Pan, Zhan-Jiang Zheng, Yue-Sheng Li\*

State Key Laboratory of Polymer Physics and Chemistry, Changchun Institute of Applied Chemistry, Chinese Academy of Sciences, Changchun 130022, China

## ARTICLE INFO

### Article history:

Received 28 August 2007  
Received in revised form 1 March 2008  
Accepted 4 March 2008  
Available online 8 March 2008

### Keywords:

Silica support  
Merrifield resin  
Nickel catalyst  
Heterogeneous catalysis  
Ethylene polymerization

## ABSTRACT

Silica and Merrifield resin were used as carriers for the support of  $\alpha$ -diimine nickel(II) precatalysts for ethylene polymerization. The  $\alpha$ -diimine ligands containing allyl were modified by introducing the reactive Si–Cl end-group, allowing their immobilization via a direct reaction of the Si–Cl groups with the silanols on silica surface or the hydroxyls on the ethanolamine-modified Merrifield resin. The resulting supported  $\alpha$ -diimine ligands were characterized by analytical and spectroscopic techniques (NMR and FT-IR). The complexation reactions of the supported ligands with  $\text{NiBr}_2(\text{dimethylether})$  (DME) gave rise to supported  $\alpha$ -diimine nickel(II) precatalysts. These heterogeneous precatalysts exhibited high activity for ethylene polymerization in the presence of modified methylaluminoxane (MMAO) as a cocatalyst. The molecular weights of the polyethylenes obtained with the supported precatalysts were much higher than those produced with the corresponding homogeneous precatalysts.

© 2008 Elsevier B.V. All rights reserved.

## 1. Introduction

Recently, there has been increasing interest in late transition metal catalysts for olefin polymerization because of the potential to yield polymers with different microstructures and the greater tolerance towards functional comonomers [1–4]. In 1995, Brookhart and coworkers discovered that aryl-substituted  $\alpha$ -diimine nickel(II) complexes in combination with different cocatalysts could polymerize ethylene with rather high activity and gave new types of polyethylene (PE) with substantial chain branching [5]. This combination of high activities and unique polymer structures make the nickel(II) catalysts desirable for applications in commercial polymerization processes. However, the application of these homogeneous catalysts in a continuous process has been difficult due to their extremely exothermic polymerization process and the serious fouling of the reactor. Thus, these catalysts need to be immobilized on suitable carriers for further applications [6–20].

One effective approach to linkage of the olefin polymerization catalysts onto the surface of carriers irreversibly is through a process of chemical tethering, and the advantage of this process is that it can prevent the catalyst from leaching out of the solid support during polymerization catalysis. This process can be achieved by two steps: modifying the surface of the support or the catalyst

structure first followed by the reaction of the reactive groups with each other to form a covalent bond. To date, a mass of literature concerning chemically tethering metallocenes have been reported [21–39]. However, there are only a few examples of tethered late transition metal catalysts [40–47].

Recently, we have developed two strategies to prepare the silica-supported bis(imino)pyridyl iron(II) catalysts through the chemical tethering [45]. When immobilized on suitable carriers, these iron catalysts showed high loadings and exhibited high activity towards ethylene polymerization. Herein we report the preparation of immobilized  $\alpha$ -diimine nickel(II) catalysts by chemical tethering, using silica or Merrifield resin as the carriers and their polymerization behavior towards ethylene polymerization in the presence of MMAO.

## 2. Experimental

### 2.1. General procedures and materials

All manipulation involving air and/or moisture-sensitive compounds was carried out with standard Schlenk techniques. The NMR data of ligands were obtained on a Bruker 300 MHz spectrometer at ambient temperature, with  $\text{CDCl}_3$  as a solvent and TMS as an internal standard. The NMR data of the polyethylenes were obtained on a Varian Unity-400 MHz spectrometer at 125 °C with  $o\text{-C}_6\text{D}_4\text{Cl}_2$  as a solvent. Infrared spectra were recorded on a Bio-Rad FTS135 spectrometer. The elemental analysis of nickel was conducted using a PerkinElmer AA800 atomic absorption

\* Corresponding author. Fax: +86 431 85262039.  
E-mail address: [ysli@ciac.jl.cn](mailto:ysli@ciac.jl.cn) (Y.-S. Li).

spectrometer. The elemental analyses of C, H, and N were performed on a Flash EA 1112 spectrometer. DSC measurements were performed with a PerkinElmer Pyris 1 differential scanning calorimeter at a heating or cooling rate of 10 °C/min. The intrinsic viscosities of the polyethylenes were measured in decalin at 135 °C using an Ubbelohed viscometer. The viscosity-average molecular weight was calculated using the following equation [48]:

$$[\eta] = 6.2 \times 10^{-4} \bar{M}_v^{0.7}$$

MMAO (7% Al in heptane solution) was purchased from Akzo Nobel Chemical Inc. Silica was purchased from Aldrich Chemicals (200 mesh, surface area: 480 m<sup>2</sup>/g), and pretreated by heating under vacuum at 150 °C for 12 h to remove the absorbed water before use. Merrifield resin (chloromethylated styrene/divinylbenzene copolymer, 3.5 mmol/g Cl, 1% cross-linked) was obtained from Aldrich. Tetrahydrofuran, hexane and toluene were purified by solvent purification system (SPS, MBraun Inertgas-Systeme GmbH). Homogeneous  $\alpha$ -diimine Ni(II) catalysts **A** (ArN=C(C<sub>10</sub>H<sub>6</sub>)C=NAr)NiBr<sub>2</sub> and **B** (ArN=C(CH<sub>3</sub>)C(CH<sub>3</sub>)=NAr)NiBr<sub>2</sub> (Ar = 2,6-*i*Pr<sub>2</sub>C<sub>6</sub>H<sub>3</sub>) were synthesized following the procedures reported in the literature [5].

### 2.2. Synthesis of ArN=C(C<sub>10</sub>H<sub>6</sub>)C=NAr (Ar = 4-allyl-2,6-*i*Pr<sub>2</sub>C<sub>6</sub>H<sub>3</sub>) **1a**

To a 250 mL flask were added acenaphthenequinone (0.91 g, 5 mmol), 4-allyl-2,6-diisopropylaniline (2.4 g, 11 mmol), and 1 mL of formic acid in 70 mL of dry methanol, and then the solution was stirred at room temperature for 18 h. A yellow solid product was isolated by filtration, washed with cold methanol, and recrystallized from ethanol, giving ligand **1a** as pale yellow crystal 2.11 g (73%). <sup>1</sup>H NMR (CDCl<sub>3</sub>):  $\delta$  7.81 (d, 2H, Nap-H), 7.30 (t, 2H, Nap-H), 6.99 (s, 4H, Ph-H), 6.57 (d, 2H, Nap-H), 6.06 (m, 2H, -CH=C), 5.07 (t, 4H, C=CH<sub>2</sub>), 3.42 (d, 4H, CH<sub>2</sub>-C=C), 2.92 (m, 4H, CH(Me)<sub>2</sub>), 1.16 (d, 24H, CH<sub>3</sub>). <sup>13</sup>C NMR (CDCl<sub>3</sub>):  $\delta$  161.17, 145.67, 140.74, 138.28, 135.47, 135.32, 131.09, 129.61, 128.73, 127.81, 123.68, 123.30, 115.33, 40.30, 28.62, 23.28. Anal. Calc. for C<sub>42</sub>H<sub>48</sub>N<sub>2</sub>: C, 86.85%; H, 8.33%; N, 4.82%. Found: C, 86.72%; H, 8.35%; N, 4.86%.

### 2.3. Synthesis of (ArN=C(CH<sub>3</sub>)-C(CH<sub>3</sub>)=NAr) (Ar = 4-allyl-2,6-*i*Pr<sub>2</sub>C<sub>6</sub>H<sub>3</sub>) **1b**

The preparation procedure is similar to that used for ligand **1a**. Yield: 76%. <sup>1</sup>H NMR (CDCl<sub>3</sub>):  $\delta$  7.01 (s, 4H, Ph-H), 5.94 (m, 2H, -CH=C), 5.10 (t, 4H, C=CH<sub>2</sub>), 3.41 (d, 4H, CH<sub>2</sub>-C=C), 2.35 (m, 4H, CH(Me)<sub>2</sub>), 1.28 (s, -CH<sub>3</sub>, 6H), 1.16 (d, 24H, CH(CH<sub>3</sub>)<sub>2</sub>). <sup>13</sup>C NMR (CDCl<sub>3</sub>):  $\delta$  16.6, 22.9, 28.6, 40.3, 115.3, 123.2, 135.0, 135.1, 138.1, 144.4, 168.4. Anal. Calc. for C<sub>34</sub>H<sub>48</sub>N<sub>2</sub>: C, 84.24%; H, 9.98%; N, 5.78%. Found: C, 84.42%; H, 9.94%; N, 4.75%.

### 2.4. Synthesis of Si-Cl modified bis(imino)acenaphthene ligand **2a**

To a 100 mL flask were added bis(imino)acenaphthene compound **1a** (2.04 g, 4 mmol), chlorodimethylsilane (2.31 g, 20 mmol) in 40 mL THF, and H<sub>2</sub>PtCl<sub>6</sub> (1 mg) as a catalyst. The reacted mixture was refluxed at 70 °C for 5 h. Excess chlorodimethylsilane and THF were removed under reduced pressure. After dried at 60 °C for 24 h in a vacuum oven, ligand **2a** (1.74 g, 75%) was obtained as yellow powder. <sup>1</sup>H NMR (CDCl<sub>3</sub>):  $\delta$  7.78 (d, 2H, Nap-H), 7.28 (t, 2H, Nap-H), 6.97 (s, 4H, Ph-H), 6.57 (d, 2H, Nap-H), 2.87 (m, 4H, CH(Me)<sub>2</sub>), 2.57 (d, 4H, Ph-CH<sub>2</sub>-), 1.75 (m, 4H, C-CH<sub>2</sub>-C), 1.3 (m, 4H, C-C-CH<sub>2</sub>), 1.18 (d, 24H, C(CH<sub>3</sub>)<sub>2</sub>), 0.5 (s, 12H, SiCH<sub>3</sub>). <sup>13</sup>C NMR (CDCl<sub>3</sub>):  $\delta$  1.3,

14.9, 22.2, 25.6, 27.6, 39.3, 122.3, 122.7, 126.1, 126.8, 127.8, 130.1, 134.4, 137.2, 139.7, 144.6, 160.2. FT-IR (cm<sup>-1</sup>): 2963, 2928, 2887, 1644, 1593, 1461, 1418, 1383, 1362, 1260, 861, 474. Anal. Calc. for C<sub>46</sub>H<sub>62</sub>Cl<sub>2</sub>N<sub>2</sub>Si<sub>2</sub>: C, 71.75%; H, 8.12%; N, 3.64%. Found: C, 71.64%; H, 8.16%; N, 3.66%.

### 2.5. Synthesis of Si-Cl modified bis(imino)butanedione ligand **2b**

The preparation procedure is similar to that used for ligand **2a**. Yield: 82%. <sup>1</sup>H NMR (CDCl<sub>3</sub>):  $\delta$  6.99 (s, 4H, Ph-H), 2.95 (m, 4H, CH(Me)<sub>2</sub>), 2.42 (d, 4H, Ph-CH<sub>2</sub>-), 1.78 (m, 8H, C-CH<sub>2</sub>-C), 1.34 (m, 4H, C-C-CH<sub>2</sub>), 1.21 (m, 24H, C(CH<sub>3</sub>)<sub>2</sub>), 0.98 (s, CH<sub>3</sub>, 6H), 0.45 (s, 12H, SiCH<sub>3</sub>). <sup>13</sup>C NMR (CDCl<sub>3</sub>):  $\delta$  1.4, 15.3, 17.1, 21.1, 23.4, 26.8, 37.4, 119.0, 133.6, 136.0, 141.4, 167.3. FT-IR (cm<sup>-1</sup>): 2960, 2932, 2886, 1643, 1573, 1460, 1435, 1383, 1364, 1254, 856, 454. Anal. Calc. for C<sub>38</sub>H<sub>62</sub>Cl<sub>2</sub>N<sub>2</sub>Si<sub>2</sub>: C, 67.72%; H, 9.27%; N, 4.16%. Found: C, 68.04%; H, 9.23%; N, 4.14%.

### 2.6. Synthesis of silica-supported $\alpha$ -bis(imine)acenaphthene **3a**

To a 100 mL flask were added Si-Cl modified ligand **2a** (0.77 g, 1 mmol), silica (heat-treated at 500 °C for 8 h) 2 g, triethylamine 5 mL, and toluene 50 mL. The mixture was refluxed for 48 h, and then cooled to room temperature. The solid was isolated by filtration, washed copiously with diethyl ether, hexane and THF, and then heated at reduced pressure to afford silica-supported  $\alpha$ -bis(imine)acenaphthene ligand **3a** 2.29 g as red powder, FT-IR (cm<sup>-1</sup>): 2968, 2937, 1633, 1469, 1435, 1385, 1103, 800. Anal. Found: C, 8.03%; N, 0.73%.

### 2.7. Synthesis of silica-supported $\alpha$ -bis(imine)butanedione **3b**

The preparation procedure is similar to that used for ligand **3a**. FT-IR (cm<sup>-1</sup>): 2965, 2872, 1638, 1472, 1435, 1385, 1101, 802. Anal. Found: C, 17.21%; N, 1.42%.

### 2.8. Synthesis of Merrifield resin supported $\alpha$ -bis(imine)acenaphthene **4a**

The preparation procedure is similar to that used for ligand **3a**. FT-IR (cm<sup>-1</sup>): 3400, 3025, 2981, 2950, 2880, 2676, 2626, 1640, 1601, 1480, 1445, 1398, 1385, 1329, 1250, 1072, 1034. Anal. Found: N, 1.53%.

### 2.9. Synthesis of Merrifield resin supported $\alpha$ -bis(imine)butanedione **4b**

The preparation procedure is similar to that used for ligand **3a**. FT-IR (cm<sup>-1</sup>): 3400, 3026, 2980, 2939, 1642, 1603, 1492, 1444, 1397, 1382, 1360, 1034. Anal. Found: N 1.84%.

### 2.10. Synthesis of silica-supported $\alpha$ -bis(imine)acenaphthene Ni(II) precatalysts **5a**

To a 100 mL flask were added silica-supported  $\alpha$ -bis(imine)acenaphthene ligand **3a** (2.0 g, 0.38 mmol) in 20 mL dichloromethane, and dimethyl ether (DME) (0.045 g, 0.5 mmol). After stirring at room temperature for 1 h, NiBr<sub>2</sub> (0.08 g, 0.38 mmol) was added. The mixture continued to be stirred for 8 h. Then the solvent was removed in a vacuum and the crude product was washed twice with diethyl ether, filtered, and dried in a vacuum to afford **5a** (1.98 g, 95%) as dark red powder. Anal. Found: C, 10.7%; H, 1.31%; N, 0.6%; Ni, 1.14%. Catalysts **5b**, **5a** and **5b** were prepared through a procedure similar to that used for **5a**.

### 2.11. Procedure for ethylene polymerization

High-pressure polymerization was carried out in a 200 mL stainless steel reactor equipped with a mechanical stirrer and internal cooling water coils. The reactor was baked under nitrogen flow for 24 h at 150 °C, subsequently cooled to the desired reaction temperature, and then purged by ethylene three times. Reagents and toluene were transferred into the reactor *via* a gastight syringe. Ethylene was introduced into the reactor, and pressure was maintained at 10 atm throughout the polymerization run by continuously feeding ethylene gas. After proceeding for 30 mins, the polymerization was stopped by turning the ethylene off and relieving the pressure. The reaction mixture was poured into a solution of HCl/ethanol (10 vol%). The polymer was isolated by filtration, washed with ethanol, and dried under vacuum at 60 °C for 24 h.

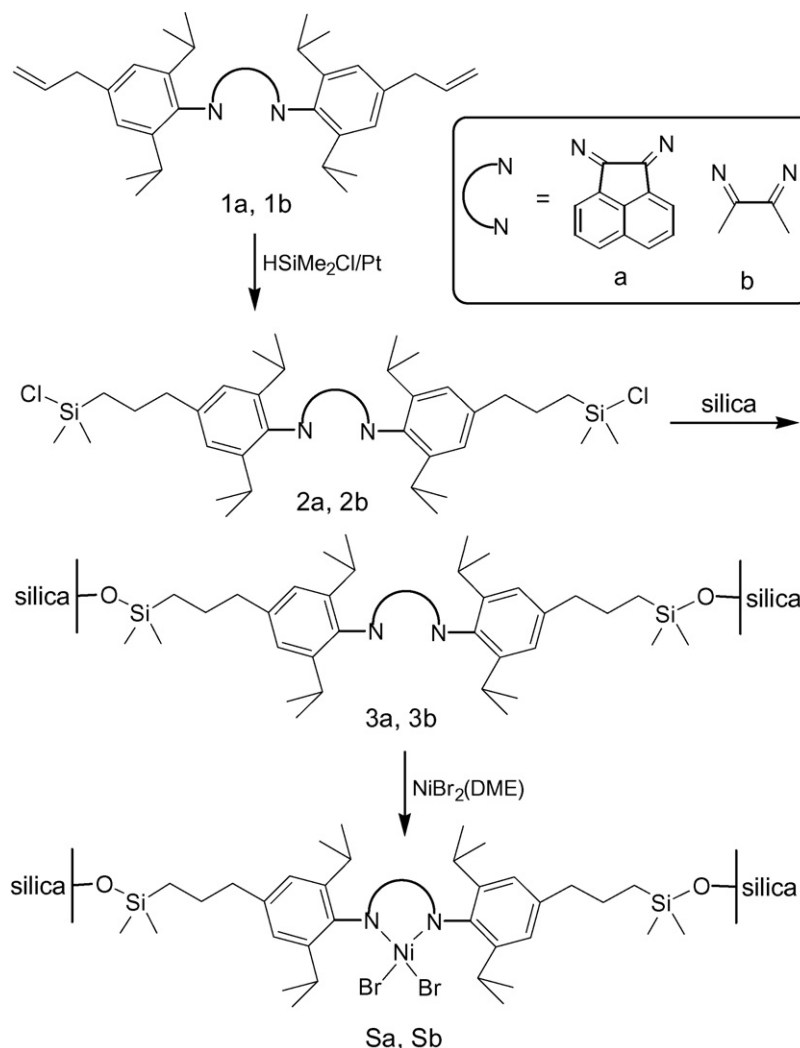
## 3. Results and discussion

### 3.1. Preparation of silica and Merrifield resin supported nickel catalysts

As shown in Scheme 1, the  $\alpha$ -diimine ligands containing allyl were prepared in good yields using the formic acid-catalyzed condensation reaction of more than two equiv. of 4-allyl-2,6-biisopropylaniline with one equiv. of acenaphthenequinone or 2,3-butanedione in methanol (yields: **1a**, 73%; **1b**, 76%). Ligands

**1a** and **1b** reacted with chlorodimethylsilane in the presence of  $\text{H}_2\text{PtCl}_6$  to afford the products containing the Si–Cl functional group, **2a** and **2b**, respectively (yields: **2a**, 75%; **2b**, 82%), and then ligands **2a** and **2b** reacted with silanols on the silica surface to produce the silica-supported  $\alpha$ -diimine ligands **3a** and **3b**, respectively. Silica-supported nickel(II) catalysts **Sa** and **Sb** were obtained as yellow powders *via* the complexation reaction of  $\text{NiBr}_2(\text{DME})$  with the corresponding silica-supported  $\alpha$ -diimine ligands **3a** and **3b**, respectively.

The silica-supported  $\alpha$ -diimine ligands were characterized *via* FT-IR and  $^{29}\text{Si}$  MAS NMR spectrum. From the FT-IR spectrum presented in Fig. 1, some characteristic features can be distinguished: for instance, the band at  $1103\text{ cm}^{-1}$  indicates the presence of Si–C bonds, the occurrence of sharp peak at  $1469\text{ cm}^{-1}$  shows the presence of  $-\text{CH}_2-$ , the peak at  $1385\text{ cm}^{-1}$  shows the presence of  $-\text{CH}_3$  group, the sharp band at  $1645\text{ cm}^{-1}$  indicates the presence of C=N, and the bands at  $2937$  and  $2968\text{ cm}^{-1}$  are attributed to  $\nu_{\text{C-H}}$  ( $-\text{CH}_3$  and  $-\text{CH}_2-$ ). The  $^{29}\text{Si}$  MAS NMR spectrum of a representative sample is shown in Fig. 2 [49]. The large  $^{29}\text{Si}$  peaks at  $-103$  and  $-111$  ppm are from the silica framework (d), and the peaks at  $-58$  and  $-68$  ppm correspond to the Si of silica linking the  $-\text{CH}_2\text{CH}_2\text{CH}_2\text{SiO}-$  group bearing OH (b) or not (c), while the peaks at  $-11$  and  $-23$  derive from the  $\text{CH}_2\text{CH}_2\text{CH}_2\text{Si}$  group (a). The immobilization of the  $\alpha$ -diimine ligands could be confirmed by the above analysis.



Scheme 1. Preparation of the silica-supported  $\alpha$ -bis(imine) nickel(II) catalysts.

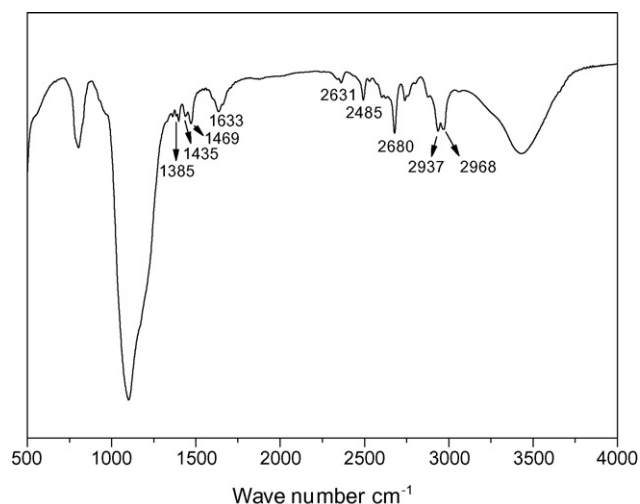


Fig. 1. FT-IR spectrum of silica-supported bis(imine) ligand **3a**.

As shown in Scheme 2, reaction of commercially available chloromethylated polystyrene-*co*-divinyl benzene beads (Merrifield resin) with an excess of ethanolamine yielded the resin containing hydroxyl [50]. The Merrifield resin supported ligands **4a** and **4b** were prepared via a procedure similar to that used for the silica-supported ligands. Through complexing with  $\text{NiBr}_2$ , the Merrifield resin supported nickel(II) catalysts **Pa** and **Pb** were obtained. The Merrifield resin supported ligands were also characterized by FT-IR. As shown in Fig. 3, the sharp peak at  $1034\text{ cm}^{-1}$  is due to the C–O bonds, the peaks at 1444, 1492 and  $1603\text{ cm}^{-1}$

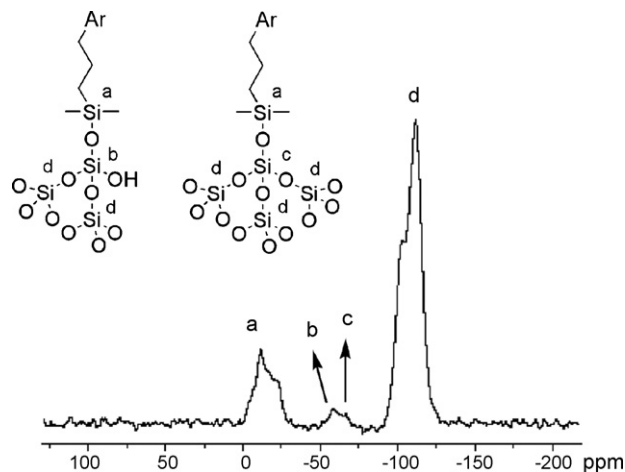
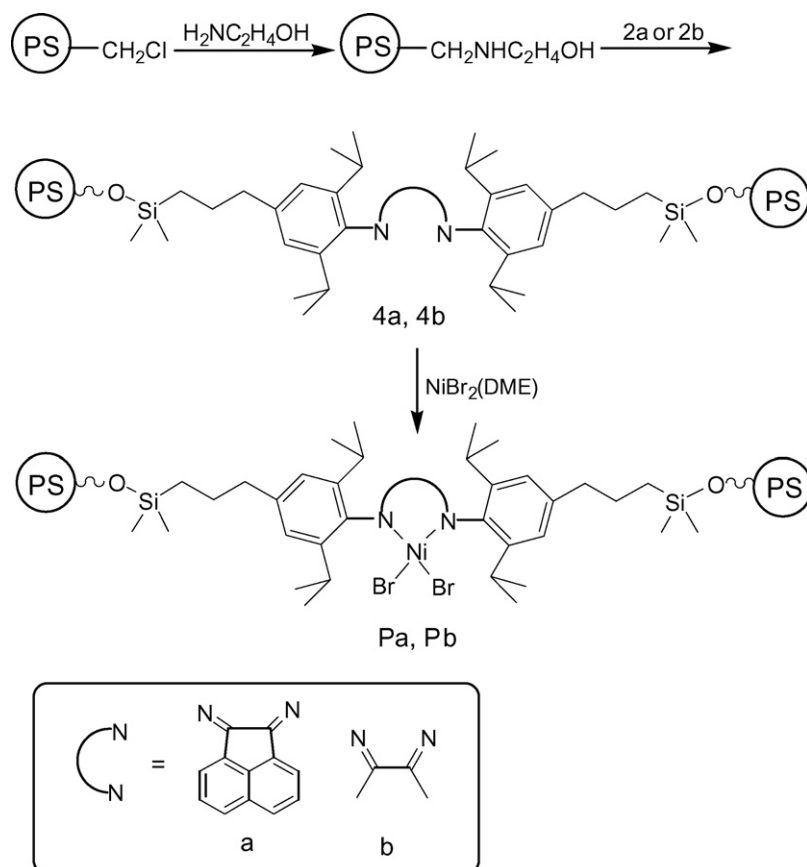


Fig. 2.  $^{29}\text{Si}$  MAS NMR spectrum of silica-supported bis(imine) ligand **3a**.

Table 1  
Results of supporting diimine nickel(II) catalysts

Precatalyst	C (%)	H (%)	N (%)	Ni (%)	Loading (mgNi/g cat)
<b>Sa</b>	10.7	1.31	0.60	1.14	11.4
<b>Sb</b>	17.2	1.19	1.12	2.23	22.3
<b>Pa</b>	–	–	1.34	2.82	28.2
<b>Pb</b>	–	–	1.74	3.93	39.3

are assigned to the benzene framework, and the peaks at 1383, 2870 and  $2960\text{ cm}^{-1}$  are from  $-\text{CH}_3$ , while the moderate peak at  $1642\text{ cm}^{-1}$  reveals the presence of C=N bonds.



Scheme 2. Preparation of the Merrifield resin supported bis(imine) nickel(II) catalysts.

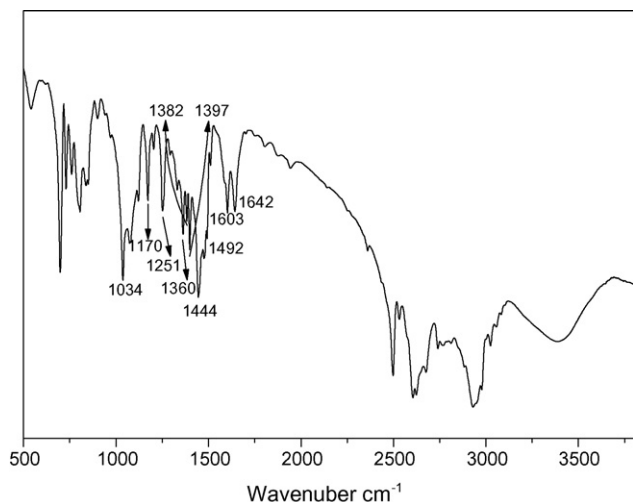


Fig. 3. FT-IR spectrum of the Merrifield resin supported bis(imine) ligand **4a**.

The loadings of nickel(II) are listed in Table 1. It is very interesting that the nickel loadings of the modified Merrifield resin are much higher than those of silica. For example, the loadings of catalysts **Pa** and **Pb** are 28.2 and 39.3 mgNi/g cat., respectively, which are almost two times those of **Sa** and **Sb**, respectively. In addition, much higher nickel loadings could be easily obtained when Si–Cl modified bis(imino)butanedione ligand **2b** with less steric effect than the corresponding Si–Cl modified bis(imino)acenaphthene ligand **2a** bearing greater steric effect was used.

### 3.2. Ethylene polymerization using the heterogenized Ni(II) precatalysts

The polymerizations of ethylene were conducted at 10 atm pressure of ethylene in toluene using immobilized precatalysts **Sa**, **Sb**, **Pa** and **Pb**, as well as the homogeneous precatalyst **A** and **B** activated with MMAO. All the immobilized catalysts showed moderate activity towards ethylene polymerization. The relationship between the Al/Ni molar ratio and the activity of the precatalysts **Sa** and **Sb** were investigated. As shown in Fig. 4, the catalyst activities increased with the increase in the Al/Ni molar ratio in the range of 100–400;

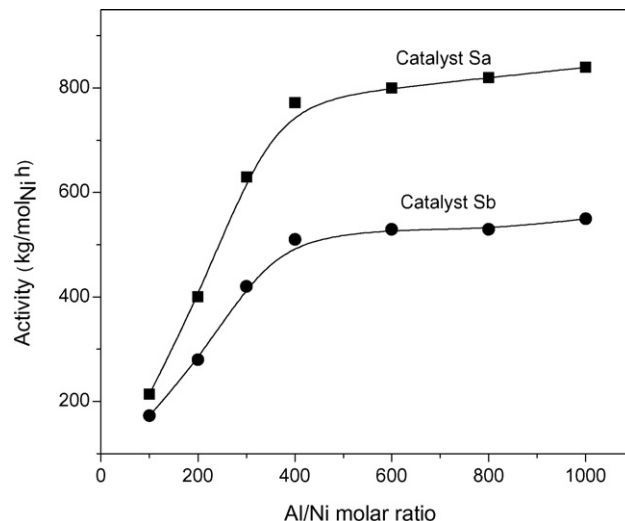


Fig. 4. Plots of catalytic activity of supported nickel(II) catalysts versus Al/Ni molar ratio. 10  $\mu$ mol Ni,  $V_{\text{total}} = 50$  mL, Ethylene pressure = 10 atm, polymerization for 30 min.

nevertheless, further increase in the Al/Ni molar ratio led to only a slight improvement of catalyst activities. The data listed in Table 2 indicated that the catalyst activities increased drastically with the increase in the Al/Ni molar ratio (e.g., Entry 4, Al/Ni = 100, the activity was 214 kg PE/mol Ni h bar; Entry 5, Al/Ni = 400, the activity was up to 772 kg PE/mol Ni h bar). In addition, the relationships among the reaction temperature and the activities of precatalysts **Sa** and **Sb** as well as the properties of the polyethylenes obtained were also investigated. As shown in Fig. 5, the rate decreased with the increase in polymerization temperature. It is possibly attributed to the poor solubility of ethylene and the deactivation of the active center at higher temperature. Like the corresponding homogeneous system, the molecular weight of the polyethylene produced by each immobilized catalyst was found to decrease as the temperature was increased (Table 2), which indicated that higher temperature led to an increase in the rate of chain transfer. The branching numbers were observed to increase with increasing reaction temperature and with a corresponding decrease in  $T_m$  values. For example, the branching numbers of the polymers obtained by catalyst **Sa**

Table 2  
The results of ethylene polymerizations with the supported Ni(II) precatalysts<sup>a</sup>

Entry	Catalyst	Al/Ni (molar ratio)	Temperature ( $^{\circ}$ C)	Activity (kg PE/mol Ni h)	Branches per 1000 C	$T_m^b$ ( $^{\circ}$ C)	$\bar{M}_v^c$ (kg/mol)
1	<b>Sa</b>	240	30	546	27.3	99.3	497
2	<b>Sa</b>	240	50	477	32.4	97.6	349
3	<b>Sa</b>	240	70	342	44.2	86.8	249
4	<b>Sa</b>	100	30	214	23.8	101.3	552
5	<b>Sa</b>	400	30	772	29.7	98.4	368
6	<b>A</b>	240	30	6350	30.3	96.8	242
7	<b>Sb</b>	240	30	347	26.3	100.7	377
8	<b>Sb</b>	240	50	311	33.1	98.3	221
9	<b>Sb</b>	240	70	230	41.9	86.4	167
10	<b>Sb</b>	100	30	180	19.2	112.3	312
11	<b>Sb</b>	400	30	508	21.1	116.7	357
12	<b>B</b>	240	30	4270	31.4	98.2	179
13	<b>Pa</b>	240	30	532	28.3	98.5	367
14	<b>Pa</b>	400	30	677	–	97.4	349
15	<b>Pa</b>	240	70	342	34.2	95.4	249
16	<b>Pb</b>	240	30	341	18.4	115.2	450
17	<b>Pb</b>	400	30	437	28.3	97.4	388
18	<b>Pb</b>	240	70	226	31.9	96.5	169

<sup>a</sup> Polymerization condition: 10  $\mu$ mol Ni,  $V_{\text{total}} = 50$  mL, polymerization under 10 atm pressure of ethylene for 30 min.

<sup>b</sup> Melting temperature determined by DSC with a heating rate of 10  $^{\circ}$ C/min in nitrogen.

<sup>c</sup> Viscosity-average molecular weights calculated from the equation  $[\eta] = 6.2 \times 10^{-4} M_v^{0.7}$  [48].

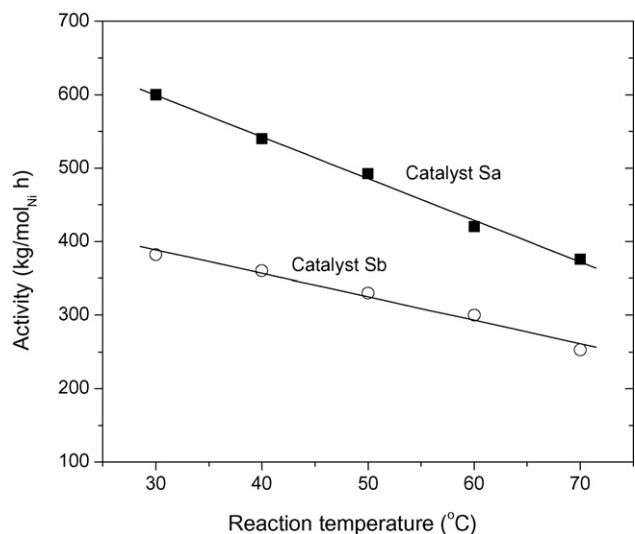


**Fig. 5.** Plots of catalytic activity of supported nickel(II) catalysts versus reaction temperature.  $10 \mu\text{mol Ni}$ ,  $V_{\text{total}} = 50 \text{ mL}$ , Ethylene pressure = 10 atm, polymerization for 30 min.

increased from 27 per thousand at  $30^\circ\text{C}$  to 44 per thousand at  $70^\circ\text{C}$ .

In general, the activities of silica-supported catalyst are about ten times as low as the activities of corresponding homogeneous catalysts (Table 2). In order to further expound this respect, we prolonged the polymerization time to 1 h; the kinetic profiles of ethylene polymerization using homogeneous catalyst A and supported precatalysts Sa/Pa are shown in Fig. 6. We found the rate profile of precatalyst A exhibits typical decay kinetics with a very high initial rate followed by a rapid decay, as shown in Fig. 6a. Although precatalyst A displays higher activity than supported systems Sa/Pa at the initial stage, the attenuation rate of the catalytic activity (or deactivation rate) of precatalyst A is much faster than that of precatalyst Sa/Pa (Fig. 6b). We thus believe that the introduction of steric bulk on the para substituents of the ligand not only block the approach of olefins, retarding the rate of associative displacement, but also decrease the rate of catalyst deactivation. The polymer produced from the supported catalyst displays much higher molecular weight than that of the

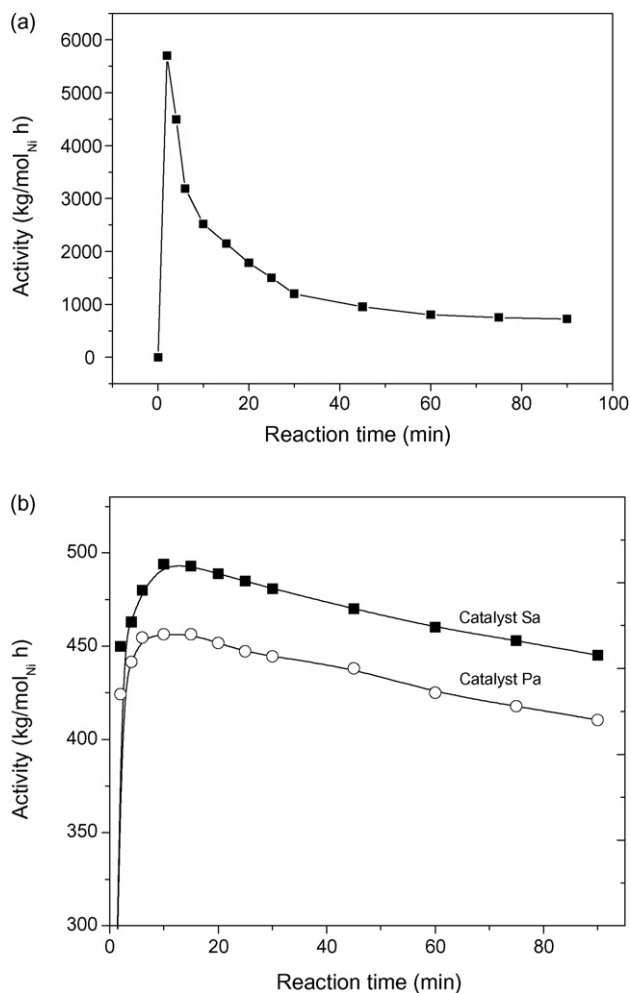


**Fig. 6.** Plots of catalytic activity of nickel(II) catalysts versus polymerization time. Polymerization reaction conditions:  $10 \mu\text{mol Ni}$ ,  $\text{Al/Ni} = 300$ ,  $V_{\text{total}} = 50 \text{ mL}$ , 10 atm ethylene,  $50^\circ\text{C}$ . (a) homogeneous catalyst A; (b) supported nickel(II) catalysts Sa and Pa.

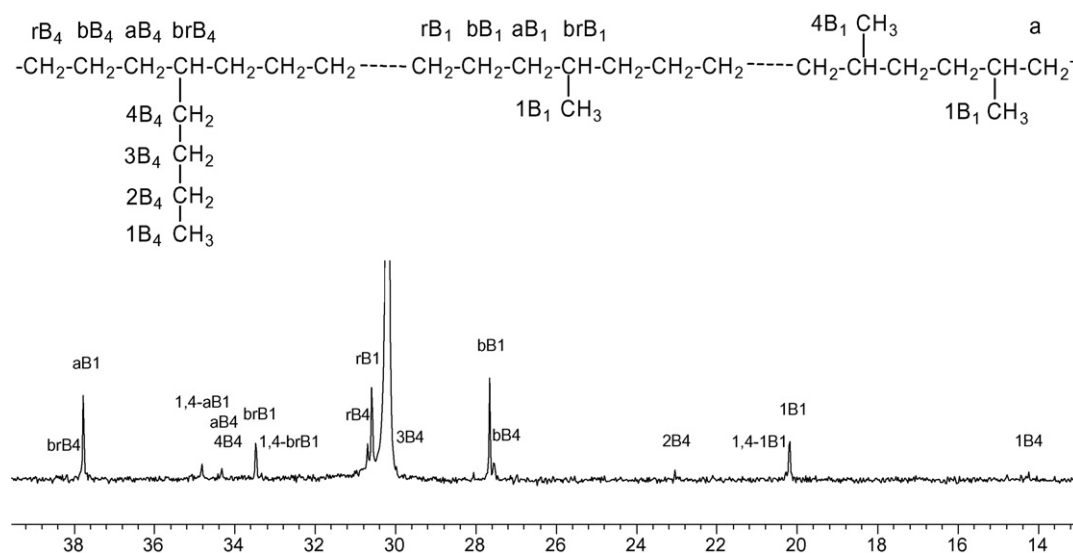


**Fig. 7.**  $^{13}\text{C}$  NMR spectrum of polyethylene prepared with catalyst Sa/MMAO at 10 atm of ethylene.

polymer made by the homogeneous catalyst (e.g., Entry 1, **Sa**,  $\bar{M}_v = 497$  kg/mol; Entry 6, **A**,  $\bar{M}_v = 242$  kg/mol; Entry 7, **Sb**,  $\bar{M}_v = 377$  kg/mol; Entry 12, **B**,  $\bar{M}_v = 179$  kg/mol). This may be ascribed to the steric surrounding from the carrier, which hinders  $\beta$ -H transfer reaction.

The branching numbers of the polymers obtained by silica-supported catalysts are slightly lower than those obtained by the corresponding homogenous catalysts. This may be ascribed to the steric surrounding from the support which hinders the chain walking rate to some extent. Thus, the polymers obtained by silica-supported catalysts display higher melting temperatures. Zhu and his colleagues found the bimodal DSC thermograms of polyethylenes when they polymerized ethylene using the silica-supported nickel-diimine catalysts. They ascribed this finding to the presence of two types of active sites: those extracted from the support during polymerization and those unextracted or kept fixed on the surface of the support [13]. It is noteworthy that our results are different from theirs, by the fact that the polymers show single melting peak in the DSC thermograms. This unique character is mainly due to the covalent bond between the catalysts to the carriers, no leaching occurring during the polymerization.

The Merrifield resin supported nickel catalysts were also employed in ethylene polymerization in the presence of MMAO at 10 atm pressure of ethylene. The results summarized in Table 2 indicate that the catalysis behavior of the Merrifield resin supported catalyst is similar to that of the silica-supported catalyst.

A typical  $^{13}\text{C}$  NMR spectrum of the polymers produced from the supported catalyst is shown in Fig. 7. The nomenclatures used for paired branches prefixes refer to the report by Galland et al. [51]. The  $^{13}\text{C}$  NMR spectrum indicates that the branches of the polyethylenes are mainly methyl branches. The presence of methyl branches was confirmed by the peaks at 37.77, 33.48, 30.59, 27.65, and 20.18 ppm, corresponding to the carbons  $aB_1$ ,  $brB_1$ ,  $rB_1$ ,  $bB_1$ , and  $1B_1$ . The signals at 34.31, 30.69, 27.55, and 23.04 ppm were corresponding to the signals of carbons  $4B_4$ ,  $rB_4$ ,  $bB_4$ , and  $2B_4$  from butyl branches. Paired 1,4 methyl branches were identified by the presence of the resonances at 20.22 ppm of 1,4- $1B_1$  carbon, and the resonance at 34.81 ppm corresponding to the 1,4- $aB_1$  carbon. No signals of ethyl and propyl branches were found. There appears no clear reason at this moment why only the methyl and butyl branches were observed in the  $^{13}\text{C}$  NMR spectrum. One possible explanation is that the reinsertion of the coordinated inner olefin of the (olefin)Ni-H species is difficult in the supported catalyst systems, and the observed butyl branches may be due to the incorporation of the simultaneously produced short chain  $\alpha$ -olefins rather than chain walking process as reported by Wu et al. [52]. We are now exploring this in more detail, and results will be available in the near future.

#### 4. Conclusions

We have synthesized a series of silica and Merrifield resin supported  $\alpha$ -diimine nickel(II) catalysts for olefin polymerization via introducing the reactive Si-Cl end-group into  $\alpha$ -diimine ligands bearing allyl groups, immobilizing them by the reaction of the Si-Cl groups with silanols on the surface of silica or the hydroxyls on the surface of modified Merrifield resin, and the complexation reaction of the supported ligands with  $\text{NiBr}_2$ . Although the initial activities of the supported catalysts are much lower than those of the corresponding homogeneous ones, the heterogeneous catalysts possess longer lifetime and still display relatively high catalytic activities towards ethylene polymerization an hour later. Furthermore, the heterogeneous catalysts also produced much higher molecu-

lar weight polymers which efficiently avoid fouling of the reactor during polymerization.

#### Acknowledgements

The authors are grateful for subsidy provided by the National Natural Science Foundation of China (Nos. 20734002 and 50525312), and by the Special Funds for Major State Basis Research Projects (No. 2005CB623800) from the Ministry of Science and Technology of China.

#### References

- [1] S.D. Ittel, L.K. Johnson, M. Brookhart, Chem. Rev. 100 (2000) 1169.
- [2] L.S. Boffa, B.M. Novak, Chem. Rev. 100 (2000) 1479.
- [3] S. Mecking, Angew. Chem. Intern. Ed. 40 (2001) 534.
- [4] B. Rieger, L.S. Baugh, S. Kacker, S. Striegler, Late Transition Metal Polymerization Catalysis, Wiley-VCH Verlag GmbH & Co., KGaA, Weinheim, 2003.
- [5] L.K. Johnson, C.M. Killian, M. Brookhart, J. Am. Chem. Soc. 117 (1995) 6414.
- [6] G.G. Hlatky, Chem. Rev. 100 (2000) 1347.
- [7] J.R. Severn, J.C. Chadwick, V.V. Castelli, Macromolecules 37 (2004) 6258.
- [8] P. Preishuber-Pflugl, M. Brookhart, Macromolecules 35 (2002) 6074.
- [9] Z. Ye, H. Alsayouri, S. Zhu, Y.S. Lin, Polymer 44 (2003) 969.
- [10] G. Braca, A.M.R. Galletti, M. Di Girolamo, G. Sbrana, R. Silla, P. Ferrarini, J. Mol. Catal. A: Chem. 96 (1995) 203.
- [11] G. Braca, M. Di Girolamo, A.M.R. Galletti, G. Sbrana, M. Brunelli, G. Bertolini, J. Mol. Catal. 74 (1992) 421.
- [12] G. Braca, G. Sbrana, A.M.R. Galletti, A. Altomare, G. Arribas, M. Michelotti, F. Ciardelli, J. Mol. Catal. A: Chem. 107 (1996) 113.
- [13] F. Alobaidi, Z. Ye, S. Zhu, Macromol. Chem. Phys. 204 (2003) 1653.
- [14] L.C. Simon, H. Patel, J.B.P. Soares, R.F. de Souza, Macromol. Chem. Phys. 202 (2001) 3237.
- [15] C.G. de Souza, R.F. de Souza, K. Bernardo-Gusmão, J. Appl. Catal. A: Gen. 325 (2007) 87.
- [16] L. Beaufort, F. Benvenuti, A.F. Noels, J. Mol. Catal. A: Chem. 260 (2006) 215.
- [17] R. Huang, N. Kukalyekar, C.E. Koning, J.C. Chadwick, J. Mol. Catal. A: Chem. 260 (2006) 135.
- [18] G. Braca, G. Sbrana, A.M. Raspolli-Galletti, A. Altomare, G. Arribas, M. Michelotti, F. Ciardelli, J. Mol. Catal. A: Chem. 107 (1996) 113.
- [19] T.R. Bousie, V. Murphy, K.A. Hall, C. Coutard, C. Dales, M. Petro, E. Carlson, H.W. Turner, T.S. Powers, Tetrahedron 55 (1999) 11699.
- [20] P. Preishuber-Pflugl, M. Brookhart, Macromolecules 35 (2002) 6074.
- [21] E.I. Iiskola, S. Timonen, T.T. Pakkanen, O. Harkki, P. Lehmus, J.V. Seppala, Macromolecules 30 (1997) 2853.
- [22] A.M. Uusitalo, T.T. Pakkanen, E.I. Iiskola, J. Mol. Catal. A: Chem. 156 (2000) 181.
- [23] A.M. Uusitalo, T.T. Pakkanen, E.I. Iiskola, J. Mol. Catal. A: Chem. 177 (2002) 179.
- [24] S. Timonen, T.T. Pakkanen, E.I. Iiskola, J. Organomet. Chem. 582 (1999) 273.
- [25] H. Schneider, G.T. Puchta, F.A.R. Kaul, G. Raudaschl-Sieber, F. Lefebvre, G. Saggio, D. Mihalios, W.A. Herrmann, J.M. Basset, J. Mol. Catal. A: Chem. 170 (2001) 127.
- [26] F. Bortolussi, J.P. Broyer, R. Spitz, C. Boisson, Macromol. Chem. Phys. 203 (2002) 2501.
- [27] (a) K. Soga, H. Kim, T. Shiono, Macromol. Chem. Phys. 195 (1994) 3347; (b) K. Soga, Macromol. Symp. 89 (1995) 249; (c) K. Soga, T. Arai, H. Nozawa, T. Uozumi, Macromol. Symp. 97 (1995) 53; (d) K. Soga, Macromol. Symp. 101 (1996) 281.
- [28] H.G. Alt, P. Schertl, A. Koppl, J. Organomet. Chem. 568 (1998) 263.
- [29] X. Cheng, O.W. Lofthus, P.A. Deck, J. Mol. Catal. 212 (2004) 121–126.
- [30] J.S. Oh, B.Y. Lee, J.E. Lee, D.H. Lee, Metallocene compounds and their use for olefin polymerization, US Patent 6,506,919 (2003) (Chem. Abstr. 133 (2000) 223183).
- [31] B.Y. Lee, J.S. Oh, Macromolecules 33 (2000) 3194.
- [32] J.S. Oh, Lee B.Y., US Patent 6,355,742 (2002) (Chem. Abstr. 131 (1999) 299823).
- [33] J. Tian, Y. Soo-Ko, R. Metcalfe, F. Yuding, S. Collins, Macromolecules 34 (2001) 3120.
- [34] J. Tian, S. Collins, US Patent 6,194,343 (2001) (Chem. Abstr. 134 (2001) 193879).
- [35] N. Suzukia, A.J. Yu, N. Shioda, H. Asami, T. Nakamura, T. Huhna, A. Fukuoka, M. Ichikawa, M. Saburi, Y. Wakatsuki, Appl. Catal. A Gen. 224 (2002) 63.
- [36] T.C. Chung, G. Xu, Y. Lu, Y. Hu, Macromolecules 34 (2001) 8040.
- [37] McNally, J. Paul, US Patent 5,767,209 (1998) (Chem. Abstr. 122 (1994) 291747).
- [38] F. Langhauser, D. Fischer, J. Kerth, Jurgen, G. Schweier, E. Barsties, H.H. Brintzinger, S. Schaible, W. Roell, US Patent 5,627,246 (1997) (Chem. Abstr. 124 (1995) 9649).
- [39] L. Mendez Llatas, A. Munoz-Escalona Lafuente, J. Campora Perez, E. Carmona Guzman, M. Lopez Reyes, Eur. Pat. Appl. 1,134,225 (2000) (Chem. Abstr. 135 (2001) 242674).
- [40] F.A.R. Kaul, G.T. Puchta, H. Schneider, F. Bielert, D. Mihalios, W.A. Herrmann, Organometallics 21 (2002) 74.
- [41] I. Kim, B.H. Han, C.S. Ha, J.K. Kim, H. Suh, Macromolecules 36 (2003) 6689.
- [42] A.M.R. Galletti, G. Geri, G. Sbrana, M. Marchionna, P. Ferrarini, J. Mol. Catal. A: Chem. 111 (1996) 273.
- [43] D. Zhang, G.X. Jin, Appl. Catal. A Gen. 262 (2004) 13.

- [44] C. Liu, G.X. Jin, *New J. Chem.* 10 (2002) 1485.
- [45] Z. Zheng, J. Liu, Y. Li, *J. Catal.* 234 (2005) 101.
- [46] H.S. Schrekker, V. Kotov, P. Preishuber-Pflugl, P. White, M. Brookhart, *Macromolecules* 39 (2006) 6341.
- [47] M. Seitz, W. Milius, H.G. Alt, *J. Mol. Catal. A: Chem.* 261 (2007) 246.
- [48] R. Chiang, *J. Polym. Sci.* 28 (1957) 235.
- [49] J. Evans, A.B. Zaki, M.Y. El-Safty, *J. Phys. Chem. B* 104 (2000) 10271.
- [50] A. Mansour, M. Portnoy, *J. Chem. Soc. Perkin Trans. 1* (2001) 952.
- [51] G.B. Galland, R.F. de Souza, R.S. Mauler, F.F. Nunes, *Macromolecules* 32 (1999) 1620.
- [52] J. Zhang, Z. Ke, F. Bao, J. Long, H. Gao, F. Zhu, Q. Wu, *J. Mol. Catal. A: Chem.* 249 (2006) 31.